Connections Between Different Types of El Niño and Southern/Northern Oscillation*

PENG Jingbei† (彭京备), ZHANG Qingyun (张庆云), and CHEN Lieting (陈烈庭)

International Center for Climate and Environment Sciences, Institute of Atmospheric Physics, Chinese Academy of Sciences, Beijing 100029

(Received May 4, 2010; in final form April 6, 2011)

ABSTRACT

It has long been acknowledged that there are two types of El Niño events, i.e., the eastern Pacific El Niño (EE) and the central Pacific El Niño (CE), according to the initial position of the anomalous warm water and its propagation direction. In this paper, the oceanic and atmospheric evolutions and the possible mechanisms of the two types of El Niño events were examined. It is found that all the El Niño events, CE or EE, could be attributed to the joint impacts of the eastward advection of warm water from the western Pacific warm pool (WPWP) and the local warming in the equatorial eastern Pacific. Before the occurrence of CE events, WPWP had long been in a state of being anomalous warm, so the strength of eastward advection of warm water was much stronger than that of EE, which played a major role in the formation of CE. While for the EE events, most contribution came from the local warming of the equatorial eastern Pacific. It is further identified that the immediate cause leading to the difference of the two types of El Niño events was the asynchronous variations of the Southern Oscillation (SO) and the Northern Oscillation (NO) as defined by Chen in 1984. When the transition from the positive phase of the NO (NO^+) to NO^- was prior to that from SO^+ to SO^-, there would be eastward propagation of westerly anomalies from the tropical western Pacific induced by NO and hence the growth of warm sea surface temperature anomalies in WPWP and its eastward propagation. This was followed by lagged SO-induced weakening of southeast trade winds and local warming in the equatorial eastern Pacific. These were conducive to the occurrence of the CE. On the contrary, the transition from SO^+ to SO^- leading the transition of NO would favor the occurrence of EE type events.

Key words: eastern Pacific El Niño, central Pacific El Niño, Southern Oscillation, Northern Oscillation

Citation: Peng Jingbei, Zhang Qingyun, and Chen Lieting, 2011: Connections between different types of El Niño and Southern/Northern Oscillation. *Acta Meteor. Sinica*, **25**(4), 506–516, doi: 10.1007/s13351-011-0409-9.

1. Introduction

According to the initial position of the warm water in the equatorial Pacific, there are two types of El Niño events (hereafter EN), namely the eastern Pacific El Niño (EE) and the central Pacific El Niño (CE; Fu et al., 1986). EE is the traditional EN, characterized by the fact that the South American coastal warming precedes the central Pacific warming, as summarized by Rasmusson and Carpenter (1982). Different from the classical one, the other type of EN, as first seen in 1982–83, is featured by the first appearance of anomalous warm water in the mid-western Pacific and its eastward propagation thereafter. This type of event has been called the CE. After 1980, CE appeared more frequently. Compared with EE, CE showed quite distinct impacts on atmospheric circulation and regional climate (Lin and Yu, 1993; Persson et al., 2005; Larkin and Harrison, 2005; Kumar et al., 2006; Weng et al., 2007; Ashok et al., 2007; Wang and Hendon, 2007; Kim et al., 2009; Lim et al., 2009; Trenberth and Smith, 2009; Taschetto et al., 2009). The horizontal structure of sea surface temperature anomaly (SSTA) and evolution of the SSTAs of CE and EE have

*Supported by the Key Technology Research and Development Program of China (2009BAC51B02), Special Public Welfare Research Fund for Meteorological Profession of China Meteorological Administration (GYHY201106015), and National Natural Science Foundation of China (40775037).

†Corresponding author: pengjingbei@mail.iap.ac.cn.

been discussed by many scientists (Fu et al., 1986; Lin, 1992; Wang, 1995; Ashok et al., 2007; Chang and Zhang, 2008; Kao and Yu, 2009). The predictability of CE and EE was also discussed (Hendon et al., 2009). However, the triggering and maintaining mechanisms for the CE have not yet been well understood. The frequent occurrence of CE was attributed to the ocean mean state changes (Wang, 1995; Kug et al., 2009), especially the shallower thermocline under the global warming (Yeh and Kirtman, 2009). Chang and Zhang (2008) discussed the zonal wind anomalies in the tropical Pacific during CE and EE. They found that the anomalous westerlies during CE events were stronger than those during EE events.

The Southern Oscillation (SO) and EN are so closely related to each other that people are prone to view them as a whole with one name of "ENSO". However, such an east-west oscillation appears not only in the southern Pacific, but also in the northern Pacific. Chen and Zhan (1984) found that there was a seesaw-like oscillation in the northern Pacific with two centers in Manila and Ship N station (30°N, 140°W) respectively at latitudes symmetric to SO, and they named this oscillation Northern Oscillation (NO). Zeng (1987) successfully simulated this dominant mode in the northern Pacific. Fu and Ye (1988) pointed out by analyzing the tropical sea level pressure (SLP) that the SO and NO could be regarded as the reflection of the interannual variability of three action centers: the equatorial low pressure zone from the Indian Ocean to western Pacific, the North Pacific high, and the South Pacific high. As the counterpart of SO, NO is closely connected with EN and SO on both interannual and interdecadal timescales (Chen, 1984, 1992). However, NO has its own characteristics. As indicated by Jin and Chen (1992), the most significant correlation between SO and SSTA appeared in the regions of Peru-Chile Current and South Equatorial Current while the most significant correlation between NO and SSTA appeared in the regions of North Equatorial Current and Equatorial Countercurrent. Moreover, the times when SO and NO reached their peaks were often not synchronous for an individual EN event. It seems to be a proper way to explore the possible mechanism behind the two types of equatorial warming through probing the evolution of SO and NO. Therefore, we will focus on the oceanic surface and subsurface evolutions for CE and EE, and in particular, their connection to the variations of SO and NO.

2. Data

The data used in this study include (1) NCEP reanalysis monthly wind at 1000 hPa (Kalnay et al., 1996) and the monthly 2°×2° standard SLP from the International Comprehensive Ocean-Atmosphere Data Set (ICOADS; Worley et al., 2005), which were downloaded from http://www.esrl.noaa.gov/psd/; (2) the observationally based Southern Oscillation index (SOI) provided by the National Oceanic and Atmospheric Administration/Climate Prediction Center (NOAA/CPC; NOAA, 2005); (3) the SSTA for the Niño-3 region obtained from NOAA/CPC at http://www.cpc.noaa.gov/data/indices/sstoi.indices. To examine the evolution of SSTA and subsurface oceanic conditions during CE and EE, we used the Kaplan Extended SSTA V2 on 5.0° latitude × 5.0° longitude (Kaplan et al., 1998) and monthly subsurface oceanic temperature anomaly (SOTA) dataset from the Joint Environmental Data Analysis Center (JEDAC) at the Scripps Institute of Oceanography on a horizontal resolution of 5°×2° in longitude and latitude and 11 vertical levels from surface to the depth of 400 m (additional information is available online at http://jedac.ucsd.edu/DATA_IMAGES/index.html). Data span the period 1951–2006, except for SOTA from 1955 to 2001. The SSTAs (and SOTAs) used in this analysis are normalized in order to highlight their variability in the western Pacific Ocean, which is generally weaker than that in the eastern Pacific Ocean.

Following the definition by Chen and Zhan (1984; also see Fu and Ye, 1988), which is similar to the definition of SOI, the NO index is defined as

$$\mathrm{NOI} = \mathrm{SLP}^*_{(25^\circ-37^\circ\mathrm{N},\ 147^\circ-135^\circ\mathrm{W})} - \mathrm{SLP}^*_{(10^\circ-17.5^\circ\mathrm{N},\ 117^\circ-123^\circ\mathrm{E})},$$

where superscript $*$ means normalized areal mean. This definition of NOI is different from the definition by Schwing et al. (2002), which is the difference between the areal mean SLP at the climatological mean position of the center of the North Pacific high and the areal mean SLP near Darwin, Australia. The two key areas involved in Schwing's definition cross the equator while our definition of NOI concentrates on the oscillation of SLP in the North Pacific.

Since we are mainly interested in variations on the interannual timescale, a 3–7-yr bandpass filter (Li, 1991) was applied to all the data to remove the short-term and interdecadal variations.

3. Definitions of EE and CE

In this paper, EE and CE are defined as the EN events with anomalous warm water originating first from the west and the east of 120°W, respectively. The definition is given according to the initial position of warm water in the tropical Pacific, similar to the definition by Fu et al. (1986) and Chang and Zhang (2008). That is to say, we classify EE and CE based on the onset phase, different from the "warm pool El Niño" and "cold tongue El Niño" (Kug et al., 2009) which were based on the peak phase of El Niño.

According to this definition, there were 6 CEs (1962, 1968, 1982, 1987, 1991, and 1997) and 4 EEs (1957, 1965, 1972, and 1977) during 1951–2001. From Fig. 1, it is seen that interdecadal changes in the frequency of CE and EE are significant. There were more EEs before the 1980s and more CEs after the 1980s. Due to this marked interdecadal change, Wang (1995) and Kug et al. (2009) attributed the occurrence of CE or EE to the difference in background ocean status.

4. Evolutions of SSTA and SOTA during EE and CE

We denote the EN developing year as year 0, the following (previous) year as year 1 (–1), and December–1 to February 0 as DJF-1. Similar to the definition of Rasmusson and Carpenter (1982), four phases for an EN event were defined: precursor (DJF-1–MAM0), development (JJA0–SON0), mature (DJF0), and decay (MAM1–JJA1).

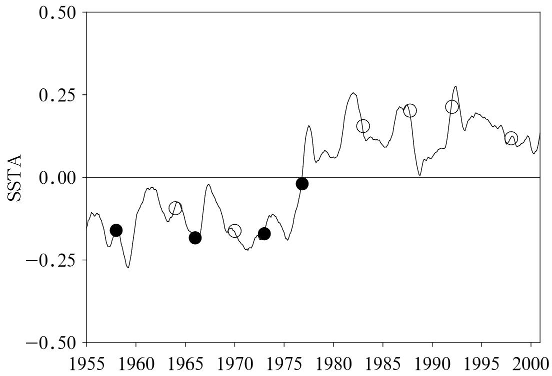

Fig. 1. Temporal evolution of 11-yr running mean of Niño-3 SSTA. Solid dots stand for EE and open circles for CE.

The evolutions of SSTAs and SOTAs of typical CE (1997) and EE (1972) events were shown in Fig. 2. From January to November 1996, before the precursor phase, there was persistent warming in the western Pacific warm pool (WPWP). The positive SSTAs extended to 160°W. During the precursor and development phases (January–July 1997), the warm water in WPWP expanded eastward, first causing the warming over the central Pacific, then the coastal warming in the Southeast Pacific. In the autumn and winter of 1997, the SSTA in the eastern tropical Pacific reached its peak. During the summer and autumn of 1998, with the invasion of cold water from WPWP, EN ended successively from the west to the east.

In the case of EE (1972), the evolution of SSTA was different. Before the precursor stage (January–October 1971), the warm water in the far western Pacific (limited to the west of 150°E) was weak and maintained quasi-stationary. There were negative SSTAs in WPWP. During the precursor and development stages (January–October 1972), the marked warm water first appeared along the southern American coast, and then propagated westward. The peak time of this EN event was the winter of 1972/1973. During the summer and autumn of 1973, with the westward propagation of cold water from the eastern Pacific, this typical EE event ended successively from the east to the west.

Examining the other five cases of CE and three cases of EE, the evolutions of SSTAs of CE (or EE) bear similarities (figures omitted). The top panels of

Fig. 3 show the composite longitude-time sections of SSTA in the equatorial Pacific for all the 6 CEs and 4 EEs, respectively. A student's t-test has been performed to determine the areas where the differences between the two composite wind fields are statistically significant at the 5% significance level (Wei, 1999). In the case of CE, the persistent warming in WPWP during the precursor stage and the eastward propagation

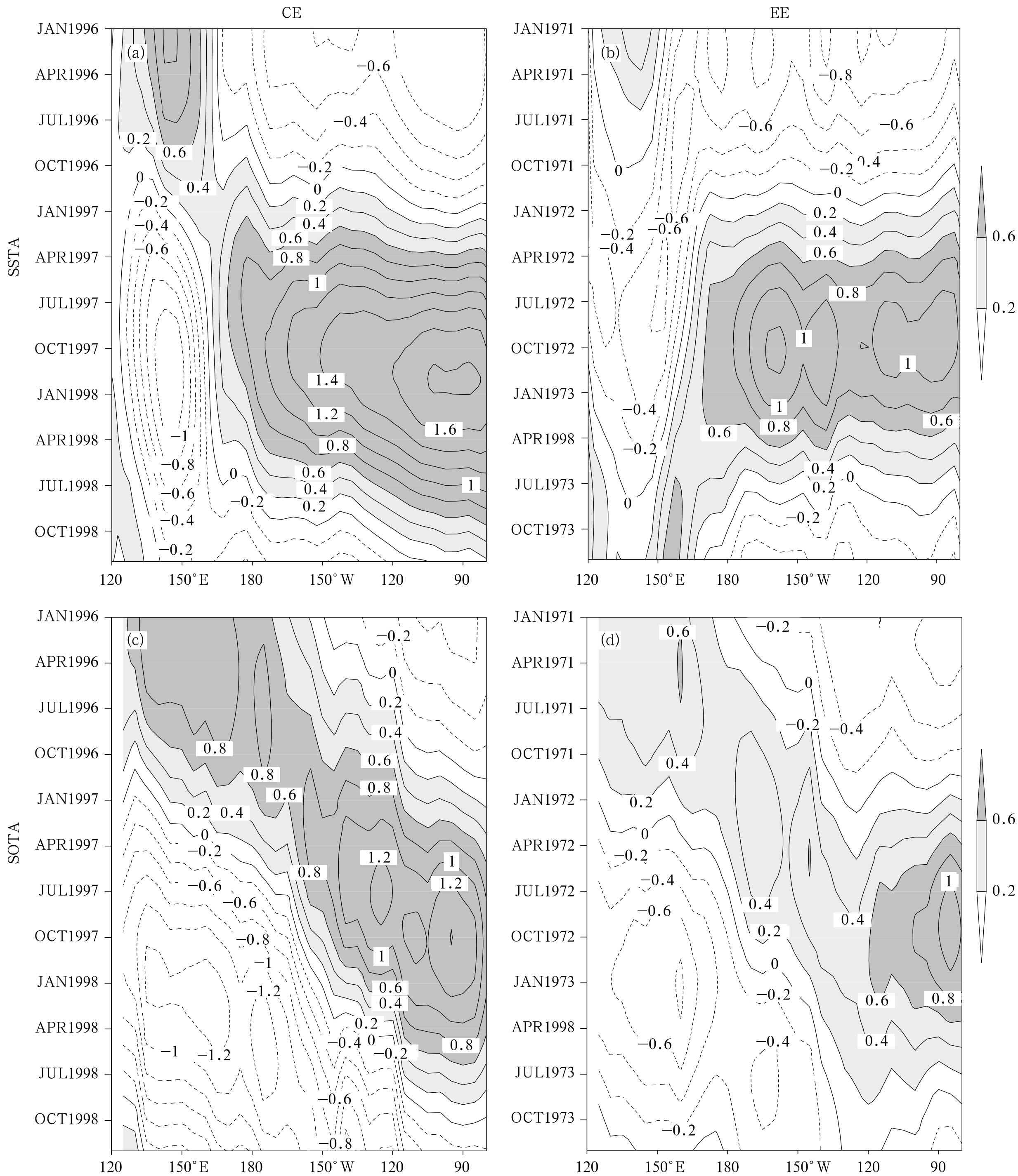

Fig. 2. Longitude-time diagrams averaged for 5°S–5°N of normalized SSTA (top panels) and SOTA (bottom panels) for the 1997 EN event (CE; left panels) and the 1972 EN event (EE; right panels). Shading denotes the area of values above the 5% significance level.

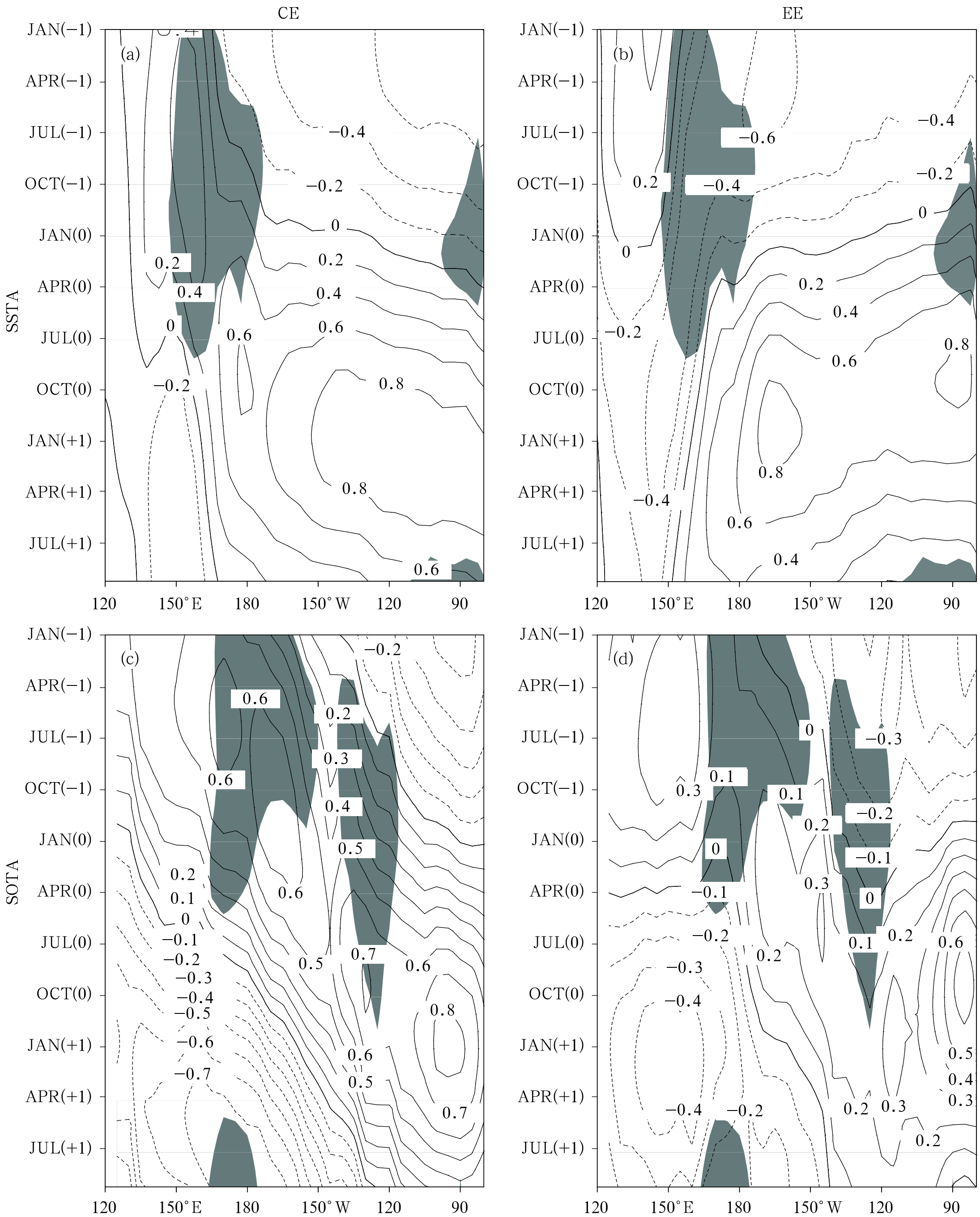

Fig. 3. Composite longitude-time diagrams averaged for 5°S–5°N of normalized SSTA (top panels) and SOTA (bottom panels) for CE (left panels) and EE (right panels) events. Shading denotes the area of values above the 5% significance level.

of warm water in the development stage were clear. The development of CE reached its peak in DJF1 followed by gradual weakening from the west to the east caused by the invasion of cold water from WPWP. In the case of EE, the warm water in the western Pacific was confined in the area west of 150°W. The SSTAs in WPWP were negative. In its onset stage (MAM0), notable warm water first appeared along the southern American coast, and then propagated westward. The peak of EE normally appeared in SON0, earlier than that of CE, which often occurred in DJF1. In the decay period (MAM1–JJA1), with the westward propagation of cold water from the eastern Pacific, the EE event was successively ending from the east to the west. Therefore, the warming in WPWP and the eastward advection of warm water thereafter from WPWP played important roles in the onset of CE while EE was mainly caused by the local anomalous warming in the equatorial eastern Pacific and the subsequent westward propagation of warm water.

The evolutions of SOTA for the cases of CE and EE (Figs. 2 and 3; bottom panels) displayed similar characteristics to SSTA, respectively. The impacts of warm water advection from WPWP and local warming in the eastern Pacific for the onsets of both CE and EE are shown more clearly.

5. Evolutions of SO and NO and their connections to CE and EE

The evolutions of SSTAs and SOTAs, as seen from Figs. 2 and 3, suggest a notable difference in the evolution of CEs and EEs. To understand the causes of the difference, let us carefully examine the evolutions of the anomalous westerlies in the tropical Pacific which could trigger EN events. In the winter of 1996/1997, the precursor stage of CE, anomalous westerlies (easterlies) prevailed over the western and central tropical Pacific (the eastern tropical Pacific) (Fig. 4a). However, before the precursor stage of EE, the autumn of 1971, the distribution of anomalous winds was different: westerly anomalies were found over the western and eastern parts of the tropical Pacific, and pronounced easterly anomalies over the central Pacific (Fig. 4b).

By examining the low-level wind anomalies over the tropical Pacific in the precursor stage of the six CE events and four EE events, we find that the differences between the two groups of events are apparently much larger than the differences among the members of each group. The composite results of the evolution of normalized winds at 1000 hPa for 6 CEs and 4 EEs are shown in Figs. 5a and 5b, respectively. In SON-1, before the onset of CE, there were two anomalous cyclonic circulations, the so-called cross-equatorial tropical cyclone pair, residing over Australia and in the east of the Philippines (Keen, 1982). Between the pair of cyclones, anomalous westerly prevailed. In the subtropical eastern Pacific, there was a pair of cross-equatorial anticyclones with anomalous easterlies prevailing in between. In fact, the positions of these anomalous cyclonic and anticyclonic vortex pairs coincided with the locations of the two atmospheric activity centers that formed SO and NO. In SON-1, SOI and NOI were both positive (Fig. 6a), and the maintenance of the anomalous cyclone over the east of the Philippines near 140°E forced persistent warming in WPWP by the anomalous southerly flow at its east flank, which provided a favorable background for the warm water advection at surface and sub-surface levels henceforth. From DJF0 to MAM0, the anomalous cyclone in the east of the Philippines migrated and extended eastward, suggesting that NO was transiting from positive phase (NO^+) to negative phase (NO^-).

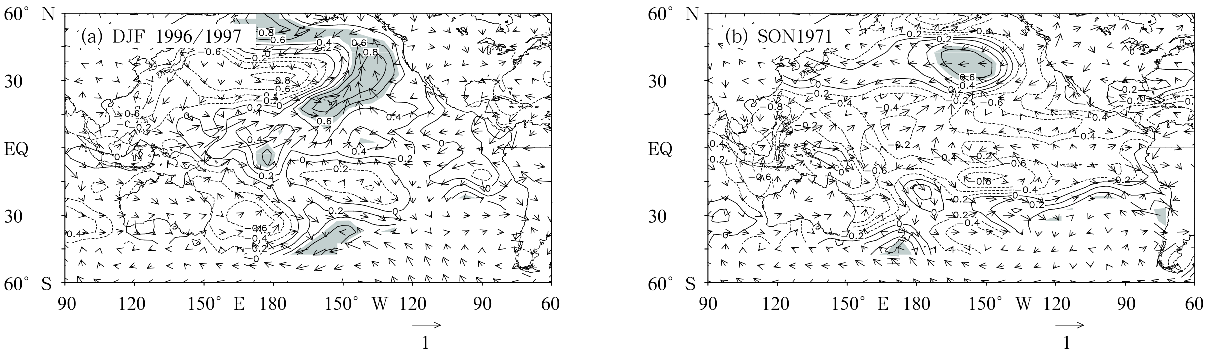

Fig. 4. Distributions of normalized winds (vectors) at 1000 hPa and normalized SSTA (contours) in the (a) winter of 1996/1997 (the precursor stage of a CE event) and (b) autumn of 1971 (before the precursor stage of an EE event). Areas with SSTA greater than 0.5 are shaded.

The anomalous westerlies along the southern flank of the anomalous cyclone also propagated eastward, enhancing the warm water advection from WPWP to eastern Pacific and leading to warming in the central Pacific (Gill, 1983; Schiller et al., 2000; Vialard et al., 2001). Meanwhile, SO remained in its positive phase (SO$^+$). Anomalous easterlies still prevailed over the equatorial eastern Pacific, being unfavorable for the coastal warming in the southeastern Pacific. Thus, two crucial scenarios for CE that occurred in sequence were: the preceding warming in WPWP associated with NO and then the local warming in the eastern Pacific caused by SO. Their joint impacts gave rise to the onset of CE. One may also see that the asynchronous progress with the transition from NO$^+$ to NO$^-$ prior to the transition of SO played a major role in the above sequence.

The main difference between the evolutions of CE and EE occurred from SON-1 to MAM0. In SON-1, the structure of SLP anomalies in North Pacific in the case of EE was similar to the one in the case of CE (figure omitted). The anomalous cyclone and anticyclone were over the western and eastern North Pacific, respectively. NO was in its positive phase. It should

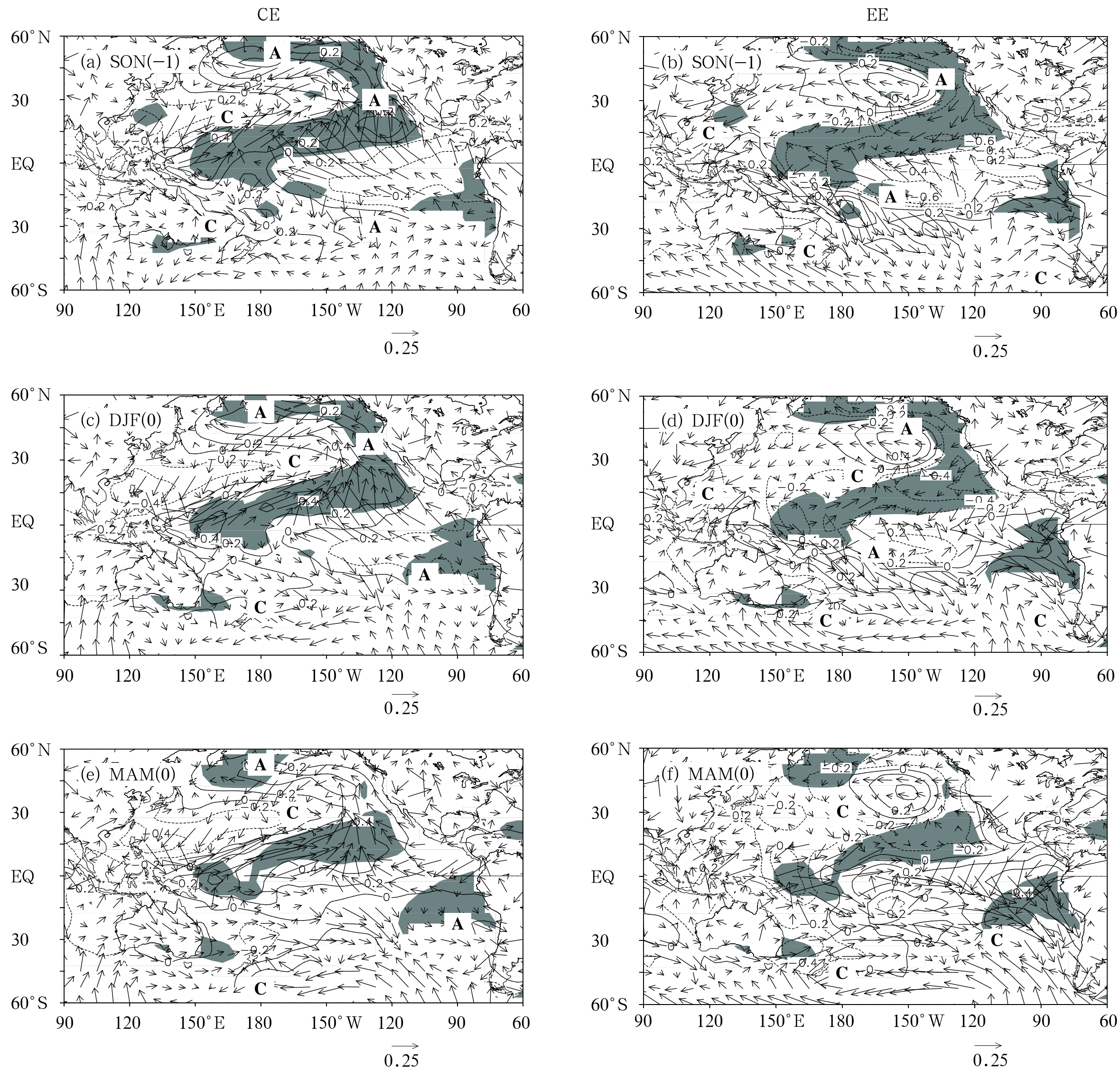

Fig. 5. Composites of SSTA (contours) and normalized winds (vectors) at 1000 hPa for CE (left panels) and EE (right panels) from SON-1 to DJF1. Areas in which the composite of SSTA differs significantly above the 5% significance level are shaded. Letter C (A) stands for the center of the anomalous cyclonic (anticyclonic) circulation.

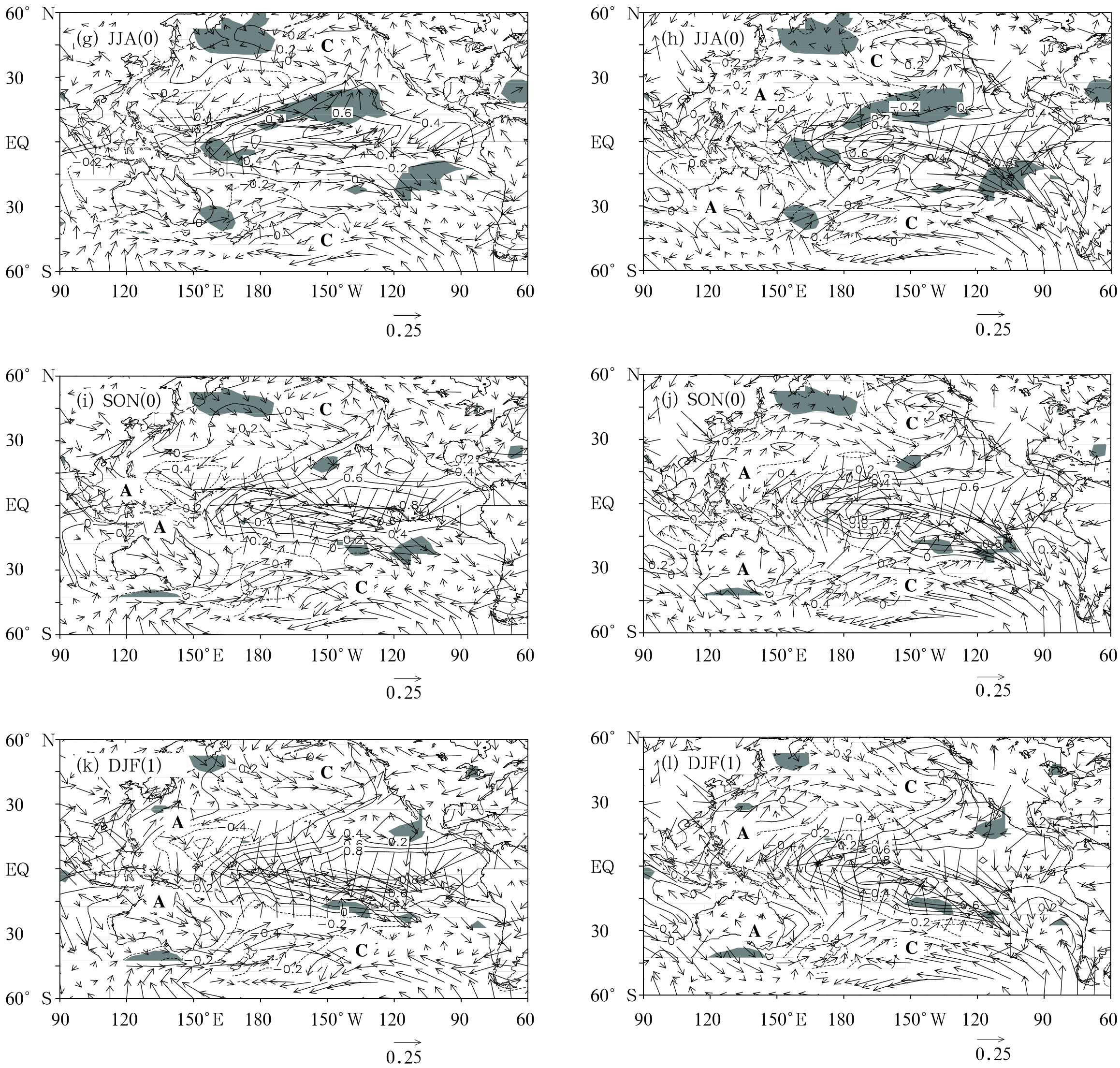

Fig. 5. (Continued.)

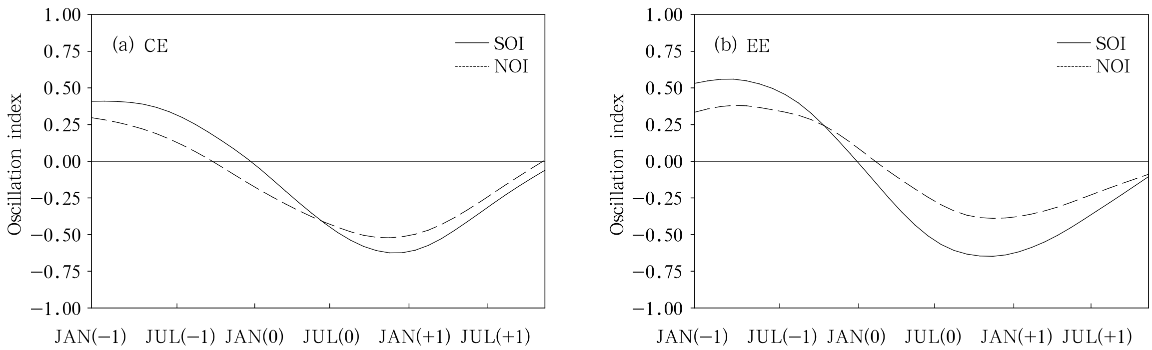

Fig. 6. Composite temporal variations of SOI (solid line) and NOI (dashed line) in the cases of CE (a) and EE (b).

be noticed that the anomalous cyclone in the northwestern Pacific was near the South China Sea, far west of its position in the case of CE. The anomalous southerly at the east flank of this anomalous cyclone led to the warming near 130°E, not in WPWP. Thus, the warm water advection from WPWP in the case of EE was weaker than in the case of CE. Meanwhile, an anomalous anticyclone was located over the central southern Pacific, and anomalous cyclones were over southeastern and southwestern Pacific, respectively. SO was in its negative phase. Wind anomalies were consistent with the SLP anomalies, with westerly anomalies over the southeastern and southwestern Pacific and easterly anomalies over the central Pacific. The relaxed southeast trade winds over the southeastern Pacific played an important role by suppressing the local upwelling, leading to the local warming (Bjerknes, 1969). The anomalous easterlies over the central Pacific restrained the warm water advection from WPWP. From DJF0 to MAM0, the anomalous cyclone over the western North Pacific extended to the central Pacific, whereas the anomalous anticyclone over the central South Pacific disappeared. NO was in its negative phase with the westerly anomalies and positive SSTA in the central Pacific. It is clear that the local warming in the eastern Pacific caused by SO was prior to the warm water advection from WPWP in the case of EE. Their joint impacts led to the onset of EE.

To summarize, the asynchronous variations of SO and NO resulted in the difference in SSTA in WPWP and the difference in the anomalous westerlies over the central and southeastern Pacific. These were two scenarios essential to the onsets of CE and EE. The composite temporal evolutions of SOI and NOI (Fig. 6) clearly show the impact of the asynchronous variations of SO and NO in the occurrences of CE and EE.

6. Conclusions

In this paper, we attempt to provide an explanation to the difference of two types of EN formation. Based on an examination of the evolutions of 10 EN events in 1951–2001, it has been shown that the eastward warm water advection from WPWP and the local warming in the southeastern Pacific both contribute to the onset of EN. We have focused on the difference of the two types of EN. For CE events, the warm water advection from WPWP played a major role, while for EE type of events the local warming process in the equatorial eastern Pacific was crucial. And before the occurrence of EN events, there was a prolonged warming process of sea water in the WPWP area for CE cases, while for EE, that tended to be a period of persistent cooling. We propose that a direct cause behind all these phenomena lies in the short-term asynchronous variations of SO and NO. For CE, the progress of NO was leading SO, and the persistent warming of sea water in WPWP as well as the subsequent stronger warm advection eastward were caused by NO (in its negative phase); the local warming in the equatorial eastern Pacific caused by SO (in negative phase; lagged) came later and worked in concert with the former. For EE, the progress of SO was leading NO and the local warming in the southeastern Pacific caused by SO (in its negative phase) was prior to the warming in the central Pacific resulted from the eastward warm water advection caused by NO (in negative phase; lagged). At the beginning of EE, there were negative SSTAs in WPWP due to NO in its positive phase. The eastward warm water advection from WPWP in the case of EE was weaker than that of CE. This may partly explain why CE tends to be always stronger than EE. These conclusions are based on the interannual variations of atmosphere and ocean. The evolutions of the original SO, NO, SSTA and SOTA (figures omitted) were similar to the corresponding ones on the 3–7-yr timescale. Thus, the asynchronous variations of SO and NO played an important role in the onsets of CE and EE.

Acknowledgments. The author would like to thank Prof. JI Liren for his helpful review on the original manuscript.

REFERENCES

Ashok, K., S. K. Behera, S. A. Rao, et al., 2007: El Niño Modoki and its possible teleconnection. *J. Geophys. Res.*, **112**, C11007, doi:10.1029/2006JC003798.

Bjerknes, J., 1969: Atmospheric teleconnections from the equatorial Pacific. *Mon. Wea. Rev.*, **97**(3), 163–172.

Chang, R., and Q. Y. Zhang, 2008: The role of the equatorial currents on the evolution of SSTA in the eastern Pacific during two different kinds of El Niño events. *Atmos. Oceanic Sci. Lett.*, **1**(1), 57–63.

Chen, L. T., 1984: The Northern Oscillation and its associations with sea-surface temperature and rainfalls over the equatorial Pacific. *Chinese Sci. Bull.*, **29**(10), 1366–1369.

——, 1992: The relationship between long-term variations in El Niño and the Northern Oscillation during the last 100 years. *Chinese Sci. Bull.*, **37**(4), 312–316.

——, and Z. Q. Zhan, 1984: Teleconnection of pressure anomalies between the eastern and western North Pacific. *Chinese Sci. Bull.*, **29**(5), 642–645.

Fu, C. B., H. F. Diaz, and J. O. Fletcher, 1986: Characteristics of the response of sea surface temperature in the Central Pacific associated with warm episodes of the Southern Oscillation. *Mon. Wea. Rev.*, **114**(9), 1716–1739.

——, and D. Z. Ye, 1988: The tropical very low-frequency oscillation on interannual scale. *Adv. Atmos. Sci.*, **5**(3), 369–388.

Gill, A. E., 1983: An estimation of sea-level and surface-current anomalies during the 1972 El Niño and consequent thermal effects. *J. Phys. Oceanogr.*, **13**(4), 586–606.

Hendon, H. H., E. Lim, G. Wang, et al., 2009: Prospects for predicting two flavors of El Niño. *Geophys. Res. Lett.*, **36**, L19713. doi:10.1029/2009GL040100.

Jin Zuhui and Chen Lieting, 1992: A comparative study on relationship of the Southern and the Northern Oscillations with the sea surface temperature in the Pacific Ocean. *Acta Oceanologica Sinica*, **14**(4), 19–27. (in Chinese)

Kalnay, E., M. Kanamitsu, R. Kistler, et al., 1996: The NCEP/NCAR 40-year reanalysis project. *Bull. Amer. Meteor. Soc.*, **77**(3), 437–471.

Kao, H. Y., and J. Y. Yu, 2009: Contrasting eastern-Pacific and central-Pacific types of ENSO. *J. Climate*, **22**(3), 615–632.

Kaplan, A., M. Cane, Y. Kushnir, et al., 1998: Analyses of global sea surface temperature 1856–1991. *J. Geophys. Res.*, **103**(C9), 18567–18589.

Keen, R. A., 1982: The role of cross-equatorial tropical cyclone pairs in the Southern Oscillation. *Mon. Wea. Rev.*, **110**(10), 1405–1416.

Kim, H. M., P. J. Webster, and J. A. Curry, 2009: Impact of shifting patterns of Pacific Ocean warming on North Atlantic tropical cyclones. *Science*, **325**(5936), 77–80.

Kug, J. S., F. F. Jin, and S. I. An, 2009: Two types of El Niño events: cold tongue El Niño and warm pool El Niño. *J. Climate*, **22**(6), 1499–1515.

Kumar, K. K., B. Rajagopalan, M. Hoerling, et al., 2006: Unraveling the mystery of Indian monsoon failure during El Niño. *Science*, **314**(5796), 115–119.

Larkin, N. K., and D. E. Harrison, 2005: On the definition of El Niño and associated seasonal average U.S. weather anomalies. *Geophys. Res. Lett.*, **32**, L13705. doi: 10.1029/2005GL022738.

Li Chongyin, 1991: *Low-Frequency Oscillation in the Atmosphere*. China Meteorological Press, Beijing, 12–18. (in Chinese)

Lim, E. P., H. H. Hendon, D. Hudson, et al., 2009: Dynamical forecast of inter-El Niño variations of tropical SST and Australian spring rainfall. *Mon. Wea. Rev.*, **137**(11), 3796–3810.

Lin Xuechun, 1992: The sea surface temperature in the North Pacific and PNA wave train. *Acta Oceanologica Sinica*, **14**(1), 29–38. (in Chinese)

——, and Yu Shuqiu, 1993: El Niño and rainfall during the flood season (June-August) in China. *Acta Meteor. Sinica*, **51**(4), 434–441. (in Chinese)

NOAA, 2005: Monthly atmospheric and sea surface temperature indices. NOAA NWS CPC [Available online at http://www. cpc. ncep. noaa. gov/data/indices/].

Persson, P. O. G., P. J. Neiman, B. Walter, et al., 2005: Contributions from California coastal-zone surface fluxes to heavy coastal precipitation: A CALJET case study during the strong El Niño of 1998. *Mon. Wea. Rev.*, **133**(5), 1175–1198.

Rasmusson, E. M., and T. H. Carpenter, 1982: Variations in tropical sea surface temperature and surface wind fields associated with the Southern Oscillation-El Niño. *Mon. Wea. Rev.*, **110**(5), 354–384.

Schiller, A., J. S. Godfrey, P. C. McIntosh, et al., 2000: Interannual dynamics and thermodynamics of the Indo-Pacific Oceans. *J. Phys. Oceanogr.*, **30**(5), 987–1012.

Schwing, F. B., T. Murphree, and P. M. Green, 2002: The Northern Oscillation index (NOI): A new climate index for the Northeast Pacific. *Progress in Oceanography*, **53**(2-4), 115–139.

Taschetto, A. S., C. C. Ummenhofer, A. S. Gupta, et al., 2009: Effect of anomalous warming in the central Pacific on the Australian monsoon. *Geophys. Res. Lett.*, **36**, L12704. doi:10.1029/2009GL038416.

Trenberth, K. E., and L. Smith, 2009: Variations in the three-dimensional structure of the atmospheric circulation with different flavors of El Niño. *J. Climate*, **22**(11), 2978–2991.

Vialard, J., C. Menkes, J.-P. Boulanger, et al., 2001: A model study of oceanic mechanisms affecting equatorial Pacific sea surface temperature during the 1997–98 El Niño. *J. Phys. Oceanogr.*, **31**(7), 1649–1675.

Wang, B., 1995: Interdecadal changes in El Niño onset in the last four decades. *J. Climate*, **8**(2), 267–285.

Wang, G., and H. H. Hendon, 2007: Sensitivity of Australian rainfall to inter-El Niño variations. *J. Climate*, **20**(16), 4211–4226.

Wei Fengying, 1999: *Modern Climatic Statistical Diagnosis and Forecasting Technology.* China Meteorological Press, Beijing, 32–33. (in Chinese)

Weng, H. Y., K. Ashok, S. K. Behera, et al., 2007: Impacts of recent El Niño Modoki on dry/wet conditions in the Pacific rim during boreal summer. *Climate Dyn.*, **29**(2-3), 113–129.

Worley, S. J., S. D. Woodruff, R. W. Reynolds, et al., 2005: ICOADS release 2.1 data and products. *Intl. J. Climatol.*, **25**, 823–842.

Yeh, S. W., and B. P. Kirtman, 2009: Internal atmospheric variability and interannual-to-decadal ENSO variability in a CGCM. *J. Climate*, **22**(9), 2335–2355.

Zeng Qingcun, 1987: The numerical simulation of climate (abstract). *Adv. Earth Sci.*, **2**, 19–22. (in Chinese)